71^{th} International Astronautical Congress (IAC) - The CyberSpace Edition, 12-14 October 2020.

IAC–20–C1,4,1,x57741

CLOSING THE LOOP BETWEEN MISSION DESIGN AND NAVIGATION ANALYSIS

Cristian Greco[a*], Massimiliano Vasile[a]

[a] *University of Strathclyde, United Kingdom*, {c.greco, massimiliano.vasile}@strath.ac.uk
[*] Corresponding author

Abstract

This research presents a contribution to the field of optimisation under uncertainty by proposing a nonlinear navigation analysis approach under both aleatoric and epistemic uncertainty. The navigation analysis is framed as a sequential filtering problem with an alternation of uncertainty propagation arcs and orbit determination instances. The state distribution is modelled as a mixture of kernels where the mixture weights are interval-valued to model the epistemic component. Specific techniques are discussed for Gaussian mixtures in particular. The uncertainty propagation step is solved by using Gaussian Hermite quadrature rules to compute the propagated means and covariances. The observation update is efficiently solved with a combination of variational inference and importance sampling, and a routine is developed to compute the posterior interval-valued weights. Given the distribution representation, lower and upper expectations of a generic quantity of interest are the solutions of linear programming problems and, therefore, are inexpensive to compute. The developed navigation analysis is finally applied to the robust quantification of the probability of impact of Europa Clipper with Jupiter's moon Europa during one of its close flybys.

Keywords: Robust Mission Design; Navigation Analysis; Epistemic Uncertainty; Variational Inference; Importance Sampling.

1. Introduction

In the mission design phase, the robustness and reliability of the reference trajectory are typically evaluated a posteriori through a navigation analysis. Thus, the trajectory design is deterministic and decoupled from the uncertainty quantification step. With this approach, numerous time-consuming iterations and handovers between the trajectory design and navigation analysis teams are needed to improve the mission robustness and reliability.

Furthermore, the navigation analysis is typically tackled as a Monte Carlo simulation of operations since diverse sources of uncertainty affect the spacecraft trajectory [13, 21]. The slow convergence is often tackled by the introduction of a number of approximations and assumptions to reduce the computational burden, e.g. dynamical linearisation and Gaussian uncertainties [6, 7, 19].

However, although the larger admissible number of samples reduces the estimator error, the estimated quantity may differ from the true sought one because of the approximations introduced. In other words, the Monte Carlo simulation may deliver accurate statistics of a possibly inaccurate operational scenario. To overcome these issues, the paradigm of mission design and analysis under uncertainty has been investigated in recent literature [4, 9, 10, 11, 14, 15, 16, 17, 22, 23].

This research presents a contribution to this modern field by proposing a nonlinear navigation analysis approach to deliver accurate statistics in a competitive computational time, i.e. such that it

can be employed directly for uncertainty quantification within trajectory optimisation. Specifically, the developed approach is constructed around a novel epistemic sequential filtering scheme, where the uncertainty is propagated directly through the nonlinear equations of motion, and updated at each observation time. Epistemic uncertainty models different observation realisations by employing a likelihood function with epistemic mean within the prior support. Furthermore, such approach can handle epistemic uncertainty over the initial and model parameters distributions. Therefore, the output distribution is obtained by directly pushing forward the input uncertainty through the navigation scenario, rather than reconstructing it by Monte Carlo simulations. This approach enables nonlinear mission analysis to be computationally tractable while solving for the true operational scenario, therefore returning more accurate estimates overall. Furthermore, the generalisation to epistemic uncertainty enables the use of a broader range of uncertainty models which may better characterise the available knowledge during the different mission design phases. The developed approach is tested for the navigation analysis of several flybys of the Europa Clipper trajectory.

The remainder of the paper is structured as follows: Section 2 is the core section of the paper presenting the novel approach for navigation analysis under epistemic uncertainty; Section 3 discusses the considered test case and presents the results obtained with the developed method; Section 4 closes the paper with the final remarks and a discussion on future developments.

2. Epistemic Navigation Analysis

In this section, a Navigation Analysis (NA) encompassing epistemic uncertainty is developed. In particular, the approach is mathematically framed as a sequential filtering problem. A typical trait of sequential filtering is the alternation of Uncertainty Propagation (UP) arcs, through the dynamical model, and Orbit Determination (OD) instances, when a new measurement is received and the state distribution is updated. The section is structured as follows: first, Section 2.1 introduces the model of epistemic uncertainty considered in this work; then, Section 2.2 describes the developed method for performing OD in the presence of epistemic uncertainty; finally, Section 2.3 presents the UP method employed in this NA approach.

2.1 Epistemic Uncertainty

Given a generic random variable $\mathbf{Z}$, we define a known family of parametric distributions with uncertain parameters $\boldsymbol{\lambda}_z$ as:

$$\mathcal{P}_z = \{p(\mathbf{z};\boldsymbol{\lambda}_z) \,|\, \boldsymbol{\lambda} \in \Omega_{\boldsymbol{\lambda}_z}\}\,, \tag{1}$$

where $\boldsymbol{\lambda}_z$ is the epistemic parameter and $\Omega_{\boldsymbol{\lambda}}$ its domain. The use of families of distributions captures the epistemic uncertainty in the knowledge of the exact probability governing the realisation of an event. Such an epistemic uncertainty can be associated with the poor characterisation of physical, e.g. celestial body's physical characteristics, or system parameters, e.g. sensor noise or engine performance. When information is sufficient to identify a single distribution, uncertainty is purely aleatory and $\Omega_{\boldsymbol{\lambda}}$ degenerate to a singleton. Therefore, Equation (1) is as a generalisation of the pure aleatoric model.

2.2 Variational Inference

Let us define $p(\mathbf{x}_k|\mathbf{y}_{1:k-1})$ the prior distribution, $p(\mathbf{y}_k|\mathbf{x}_k)$ the likelihood function of the received observation and $p(\mathbf{x}_k|\mathbf{y}_{1:k})$ the sought posterior. By Bayesian inference, the target distribution is [18]

$$p(\mathbf{x}_k|\mathbf{y}_{1:k}) = \frac{p(\mathbf{y}_k|\mathbf{x}_k)\, p(\mathbf{x}_k|\mathbf{y}_{1:k-1})}{p(\mathbf{y}_k|\mathbf{y}_{1:k-1})}\,, \tag{2}$$

where

$$p(\mathbf{y}_k|\mathbf{y}_{1:k-1}) = \int p(\mathbf{y}_k|\mathbf{x}_k)\, p(\mathbf{x}_k|\mathbf{y}_{1:k-1})\, d\mathbf{x}_k.$$

The Bayes update process is represented in Figure 1, where the prior is represented in blue, the

likelihood in yellow and the posterior in green. The denominator is the most complex term to

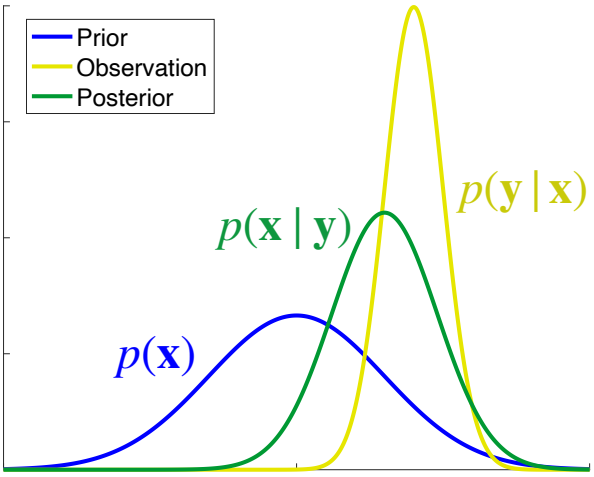

Fig. 1: Representation of Bayes' inference.

compute as it requires solving a multidimensional integral. Hence, the goal is to approximate $p(\mathbf{x}_k|\mathbf{y}_{1:k})$ with a parametric variational distribution $q(\mathbf{x}_k)$.

2.2.1 *Variational Distribution Optimisation*

We use KL divergence as measure of dissimilarity between target p and variational distribution q

$$\begin{aligned} D_{KL}(p\|q) &= \mathbb{E}_q\left[\ln \frac{q(\mathbf{x}_k)}{p(\mathbf{x}_k|\mathbf{y}_{1:k})}\right] \\ &= \int \ln \frac{q(\mathbf{x}_k)}{p(\mathbf{x}_k|\mathbf{y}_{1:k})}\, q(\mathbf{x}_k)\, d\mathbf{x}_k\,, \end{aligned} \tag{3}$$

where $\mathbb{E}_q$ indicates the expectation with respect to q. The goal is therefore to find the variational distribution minimising the divergence

$$q^*(\mathbf{x}_k) = \arg\min_{q\in\mathcal{Q}} D_{KL}(p\|q), \tag{4}$$

where $\mathcal{Q}$ is the set of admissible variational distributions. To simplify the optimisation, the divergence can be written by exploiting logarithmic properties as

$$D_{KL}(p\|q) = \mathbb{E}_q\left[\ln q(\mathbf{x}_k) - \ln p(\mathbf{x}_k|\mathbf{y}_{1:k})\right]\,. \tag{5}$$

Substituting Equation (2) and using the expectation linearity, one gets

$$\begin{aligned} D_{KL}(p\|q) &= \mathbb{E}_q\left[\ln \frac{q(\mathbf{x}_k)}{p(\mathbf{y}_k|\mathbf{x}_k)\, p(\mathbf{x}_k|\mathbf{y}_{1:k-1})}\right] + \\ &\quad \mathbb{E}_q\left[\ln p(\mathbf{y}_k|\mathbf{y}_{1:k-1})\right] \\ &= \mathbb{E}_q\left[\ln \frac{q(\mathbf{x}_k)}{p(\mathbf{y}_k|\mathbf{x}_k)\, p(\mathbf{x}_k|\mathbf{y}_{1:k-1})}\right] + \\ &\quad \ln p(\mathbf{y}_k|\mathbf{y}_{1:k-1})\,, \end{aligned} \tag{6}$$

where $\mathbb{E}_q\left[\ln p(\mathbf{y}_k|\mathbf{y}_{1:k-1})\right] = \ln p(\mathbf{y}_k|\mathbf{y}_{1:k-1})$ because $\ln p(\mathbf{y}_k|\mathbf{y}_{1:k-1})$ is independent from $\mathbf{x}$. Therefore, $\ln p(\mathbf{y})$ is a constant and can be neglected in the optimisation, which can now be written as

$$\min_{q\in\mathcal{Q}} \mathbb{E}_q\left[\ln \frac{q(\mathbf{x}_k)}{p(\mathbf{y}_k|\mathbf{x}_k)\, p(\mathbf{x}_k|\mathbf{y}_{1:k-1})}\right]\,. \tag{7}$$

In general, the expectation has no closed-form solution and needs to be computed numerically. As the expectation is a n-dimensional integral, employing an efficient numerical method is crucial in solving efficiently the minimisation problem. In this paper, we employ importance sampling to the expectation computation, that is a Monte Carlo method sampling a proposal distribution $\pi(\mathbf{x}_k)$ which has a larger support than all the distributions in $\mathcal{Q}$. Hence, we can rewrite the generic expectation $\mathbb{E}_q\left[\phi(\mathbf{x}_k)\right]$ as

$$\begin{aligned} \mathbb{E}_q\left[\phi(\mathbf{x}_k)\right] &= \int \phi(\mathbf{x}_k)\, q(\mathbf{x}_k)\, d\mathbf{x}_k \\ &= \int \phi(\mathbf{x}_k)\, \frac{q(\mathbf{x}_k)}{\pi(\mathbf{x}_k)}\, \pi(\mathbf{x}_k)\, d\mathbf{x}_k \\ &= \mathbb{E}_\pi\left[\phi(\mathbf{x}_k)\, \frac{q(\mathbf{x}_k)}{\pi(\mathbf{x}_k)}\right]\,. \end{aligned} \tag{8}$$

Thus, a Monte Carlo method taking N samples from the proposal $\mathbf{x}_k^{(i)} \sim \pi(\mathbf{x}_k)$ approximates the posterior as

$$\mathbb{E}_q\left[\phi(\mathbf{x}_k)\right] \approx \frac{1}{N}\sum_{i=1}^{N} \frac{q(\mathbf{x}_k^{(i)})}{\pi(\mathbf{x}_k^{(i)})}\, \phi(\mathbf{x}_k^{(i)})\,. \tag{9}$$

Therefore, we can run the optimisation over the variational distributions using a single proposal and fixed samples. Furthermore, many of the quantities are now independent on q and therefore can be precomputed. The discretised optimisation problem to be solved now is

$$\min_{q\in\mathcal{Q}} \sum_{i=1}^{N} \frac{q(\mathbf{x}_k^{(i)})}{\pi(\mathbf{x}_k^{(i)})} \ln \frac{q(\mathbf{x}_k^{(i)})}{p(\mathbf{y}_k|\mathbf{x}_k^{(i)})\, p(\mathbf{x}_k^{(i)}|\mathbf{y}_{1:k-1})} . \tag{10}$$

2.2.2 *Epistemic Variational Inference*

In the epistemic setting, both the prior distribution, coming from the propagation, and the likelihood function can be affected by epistemic uncertainty as

$$\begin{matrix} p(\mathbf{x}_k|\mathbf{y}_{1:k-1};\boldsymbol{\lambda}_{x_k}) \in \mathcal{P}_{x_k} \\ p(\mathbf{y}_k|\mathbf{x}_k;\boldsymbol{\lambda}_{y_k}) \in \mathcal{P}_{y_k} \end{matrix} . \tag{11}$$

The posterior distribution resulting from the variational inference (4) is therefore set-valued as well

$$q(\mathbf{x}_k;\boldsymbol{\lambda}_{x_k},\boldsymbol{\lambda}_{y_k}) \in \mathcal{P}_{x_k|y_k} \tag{12}$$

with

$$\mathcal{P}_{x_k|y_k} = \left\{ q^*(\mathbf{x}_k;\boldsymbol{\lambda}_{x_k},\boldsymbol{\lambda}_{y_k}) \;\middle|\; \arg\min_{q\in\mathcal{Q}} D_{KL}\left(p(\mathbf{x}_k|\mathbf{y}_{1:k};\boldsymbol{\lambda}_{x_k},\boldsymbol{\lambda}_{y_k}) \,\|\, q(\mathbf{x}_k)\right) \right\} . \tag{13}$$

The disadvantage of this representation is that the epistemic uncertainty accumulates when new observations are received leading to an increase in the uncertainty space dimensionality.

Hence, we aim at constructing a posterior set representation as

$$q(\mathbf{x}_k;\boldsymbol{\lambda}_{x_k|y_{1:k}}) \in \mathcal{P}_{x_k|y_{1:k}} , \tag{14}$$

which is therefore independent on $\boldsymbol{\lambda}_{x_k}$ and $\boldsymbol{\lambda}_{y_k}$ once the inference step is completed. To achieve this goal, the variational distribution employed is a mixture one as

$$q(\mathbf{x}_k;\boldsymbol{\lambda}_{x_k|y_{1:k}}) = \sum_{j=1}^{M} \lambda_{x_k|y_{1:k}}^{(j)} q^{(j)}(\mathbf{x}_k) \tag{15}$$

subject to

$$\begin{aligned} &\sum_{j=1}^{M} \lambda_{x_k|y_{1:k}}^{(j)} = 1 \\ &\int q^{(j)}(\mathbf{x}_k) d\mathbf{x}_k = 1 \;\; \forall j \in [1,\dots,M] . \end{aligned} \tag{16}$$

The conditions (16) ensures that the distribution (17) is a valid density function integrating to one. The epistemic parameters are the mixture weights

$$\boldsymbol{\lambda}_{x_k|y_{1:k}} = [\lambda_{x_k|y_{1:k}}^{(1)},\dots,\lambda_{x_k|y_{1:k}}^{(M)}] . \tag{17}$$

Thus, the variational optimisation (4) should be carried out including a linear constraint on the parameters sum

$$\begin{aligned} \min_{\boldsymbol{\lambda}_{x_k|y_{1:k}}} \sum_{i=1}^{N} \Bigg[&\frac{\sum_{j=1}^{M} \lambda_{x_k|y_{1:k}}^{(j)} q^{(j)}(\mathbf{x}_k^{(i)})}{\pi(\mathbf{x}_k^{(i)})} \cdot \\ &\ln \frac{\sum_{j=1}^{M} \lambda_{x_k|y_{1:k}}^{(j)} q^{(j)}(\mathbf{x}_k^{(i)})}{p(\mathbf{y}_k|\mathbf{x}_k^{(i)})\, p(\mathbf{x}_k^{(i)}|\mathbf{y}_{1:k-1})} \Bigg] \\ \text{s.t.} \quad &\sum_{j=1}^{M} \lambda_{x_k|y_{1:k}}^{(j)} = 1 \quad . \end{aligned} \tag{18}$$

Hence, the procedure to perform the variational inference under epistemic uncertainty is structured as follows:

1. Take S different pairs of prior and likelihood epistemic parameters $\boldsymbol{\lambda}_{x_k} \in \Omega_{\boldsymbol{\lambda}_{x_k}}$ and $\boldsymbol{\lambda}_{y_k} \in \Omega_{\boldsymbol{\lambda}_{y_k}}$;

2. For each s-th pair of epistemic parameters, with $s = 1,\dots,S$, solve the optimisation (18) to get the optimal coefficients $\boldsymbol{\lambda}_{x_k|y_{1:k}}^{s*}$;

3. Construct the posterior epistemic set as

$$\mathcal{P}_{x_k|y_k} = \Big\{ \sum_{j=1}^{M} \lambda^{(j)}_{x_k|y_{1:k}} q^{(j)}(\mathbf{x}_k) \;\Big|\; \lambda^{(j)}_{x_k|y_{1:k}} \in \Big[\min_s \lambda^{s*(j)}_{x_k|y_{1:k}}, \max_s \lambda^{s*(j)}_{x_k|y_{1:k}} \Big], \sum_{j=1}^{M} \lambda^{(j)}_{x_k|y_{1:k}} = 1 \Big\}. \tag{19}$$

The posterior epistemic set is therefore constructed by taking an outer approximation on the coefficients found by performing variational inference on S epistemic instances of the prior and likelihood.

Such process is illustrated in Figure 2. Specifically, Figure 2(a) represents the kernels $q^{(j)}(\mathbf{x}_k)$ of the variational distribution. Figure 2(b) depicts the posteriors with coefficients $\boldsymbol{\lambda}^{s*}_{x_k|y_{1:k}}$ resulting from the S variational inferences performed. Once the epistemic posterior is formed as in Equation (19), Figure 2(c) represents multiple instances of such posterior obtained by sampling the epistemic coefficients within the component-wise bounds $\left[\min_s \lambda^{s*(j)}_{x_k|y_{1:k}}, \max_s \lambda^{s*(j)}_{x_k|y_{1:k}}\right]$ under the conditions that they sum to one.

Such epistemic inference enables the re-initialisation of the state uncertainty after each observation update. The posterior imprecise set is indeed constructed with epistemic parameters $\boldsymbol{\lambda}_{x_k|y_{1:k}}$ which do not depend on the previous history. Therefore, this procedure avoids the aforementioned accumulation of uncertainty.

The optimisation in Equation (18) is performed using a local solver because analytical derivatives of the objective are available and easy to compute and the constraints are linear. It may be the case that the global optimum is not found, however the goal is to select a variational distribution which suitably approximates the target posterior, although not the best possible fit. Therefore, local optimality is considered acceptable because of the advantages in computational time.

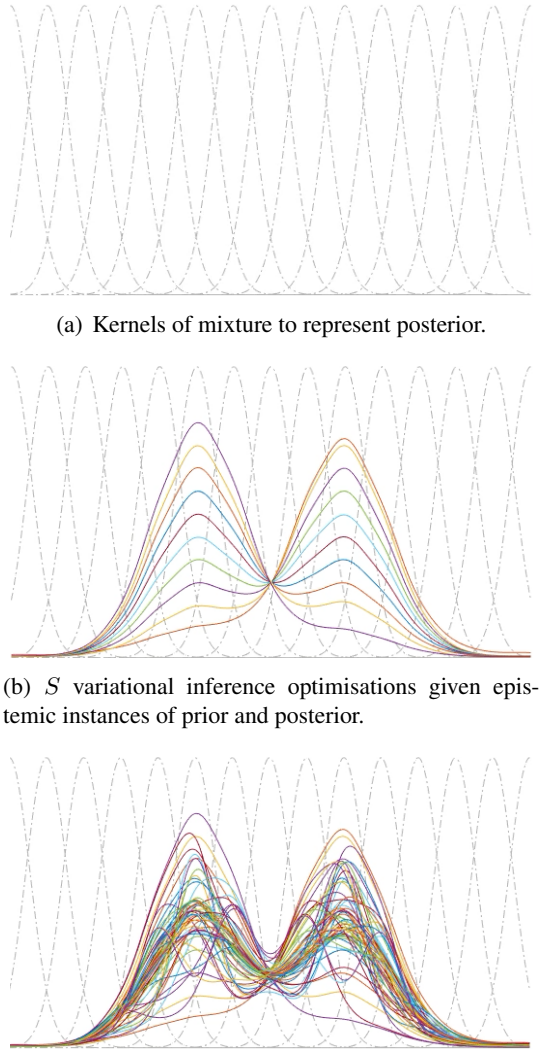

(a) Kernels of mixture to represent posterior.

(b) S variational inference optimisations given epistemic instances of prior and posterior.

(c) Instances of the epistemic posterior distribution (19).

Fig. 2: Representation of the epistemic variational inference approach.

The derivative of the objective with respect to the j-th free variable is

$$\sum_{i=1}^{N} \left[\frac{q^{(j)}(\mathbf{x}^{(i)}_k)}{\pi(\mathbf{x}^{(i)}_k)} \cdot \left(\ln \frac{\sum_{j=1}^{M} \lambda^{(j)}_{x_k|y_{1:k}} q^{(j)}(\mathbf{x}^{(i)}_k)}{p(\mathbf{y}_k|\mathbf{x}^{(i)}_k)\, p(\mathbf{x}^{(i)}_k|\mathbf{y}_{1:k-1})} + 1 \right) \right]. \tag{20}$$

Hence, the analytical objective's gradient can be

easily computed.

2.3 Uncertainty Propagation

The state UP in time is a computationally intensive step. Therefore, usually, some approximations are enforced to speed up the UP, such as linearisation of the dynamics and Gaussian-assumed uncertainty distributions [7, 19, 20]. In this work, we aim at employing a method which keeps the dynamical nonlinearities and employing a more complex distribution parameterisation. In the epistemic inference developed, the variational distribution has been imposed to be a mixture of kernels. In this section, we will focus on UP for a mixture of normal distributions, although different kernels can be easily adapted. Specifically, we will shortly describe the approach introduced in [9] specializing it for Gaussian mixtures.

The approach splits the UP into two fundamental steps: first, a polynomial representation of all the possible states at time t_k given the states at time t_{k-1}, the uncertain parameters and the control variables; then, the distributions at time t_{k-1} are sampled and propagated through the polynomial mapping to construct the distribution at time t_k. This second step requires only multiple inexpensive evaluations of the polynomial, therefore a high number of samples can be employed.

2.3.1 Sparse Polynomial Mapping

Consider the set $\Omega_{\boldsymbol{\xi}_{k-1}}$ of all possible uncertainty realisations $\boldsymbol{\xi}_{k-1} = [\mathbf{x}_{k-1}, \mathbf{u}_{k-1}]^T$ at time t_{k-1}, where $\mathbf{u}_{k-1}$ are realisations of an uncertain control action. The set $\mathcal{F}_k^{k+1}$ of compatible states at time t_{k+1} can be defined as

$$\mathcal{F}_{k-1}^{k} = \{\mathbf{x}_k(\boldsymbol{\xi}_{k-1}) \,|\, \boldsymbol{\xi}_{k-1} \in \Omega_{\boldsymbol{\xi}_{k-1}}\} \,, \tag{21}$$

where $\mathbf{x}_k(\boldsymbol{\xi}_{k-1})$ is defined as

$$\mathbf{x}_k(\boldsymbol{\xi}_{k-1}) = \mathbf{x}_{k-1} + \int_{t_{k-1}}^{t_k} f(t, \mathbf{x}, \mathbf{u}_{k-1}) \; dt \,, \tag{22}$$

where f represents the set of ordinary differential equations governing the spacecraft motion

$$\dot{\mathbf{x}} = f(t, \mathbf{x}, \mathbf{u}) \,. \tag{23}$$

The polynomial relationship which connects the set $\Omega_{\boldsymbol{\xi}_{k-1}}$ to $\mathcal{F}_{k-1}^{k}$ can be written as

$$F_{k-1}^{k}(\boldsymbol{\xi}_{k-1}) \approx \sum_{i=0}^{N_q} \alpha_{k,i} \, \Psi_i(\boldsymbol{\xi}_{k-1}) \;\; \forall \boldsymbol{\xi}_{k-1} \in \Omega_{\boldsymbol{\xi}_{k-1}} \tag{24}$$

where Ψ_i is the i-th multivariate polynomial basis and $\alpha_{k,i}$ its coefficient. The expansion is truncated to a finite order q, with corresponding N_q multivariate basis, to handle it numerically.

In this work the coefficients $\alpha_{k,i}$ are computed by stochastic collocation [2]: a number of responses $\mathbf{x}_k^{(j)}$ is evaluated over a structured grid of collocation samples $\boldsymbol{\xi}_{k-1}^{(j)}$; then a polynomial representation F_{k-1}^{k} is fitted the set of propagated samples. A sparse Smolyak collocation is employed to limit the grid dimensionality growth with increasing uncertain dimensions.

2.3.2 Gaussian Mixture Propagation

In the developed approach, the state probability distribution $p(\mathbf{x}_{k-1})$ at time t_{k-1} is a Gaussian mixture one with interval-valued weights (see eq. (19))

$$p(\mathbf{x}_{k-1}) = \sum_{j=1}^{M} \lambda_{k-1}^{(j)} \, \mathcal{N}(\mathbf{x}_{k-1}; \boldsymbol{\mu}_{k-1}^{(j)}, \boldsymbol{\Sigma}_{k-1}^{(j)}) \,, \tag{25}$$

where $\boldsymbol{\lambda}_{k-1}$ is used to abbreviate $\boldsymbol{\lambda}_{x_{k-1}|y_{1:k-1}}$ for ease of notation, $\boldsymbol{\mu}^{(j)}$ is the j-kernel mean and $\boldsymbol{\Sigma}^{(j)}$ its covariance. The goal is to compute the propagated distribution $p(\mathbf{x})$ at time t_k.

In general, an uncertainty distribution propagated through a nonlinear dynamics does not keep its Gaussianity. However, when using a Gaussian mixture, each kernel acts on a more localised portion of the domain. Therefore, the dynamical nonlinearities experienced in each component are

smaller than they would have been by using a single larger Gaussian distribution.

Hence, the propagated distribution is still assumed as a Gaussian mixture in the form of

$$p(\mathbf{x}_k) = \sum_{j=1}^{M} \lambda_{k-1}^{(j)} \mathcal{N}(\mathbf{x}_k; \boldsymbol{\mu}_k^{(j)}, \boldsymbol{\Sigma}_k^{(j)}) \,, \quad (26)$$

where the means and covariances are computed as

$$\begin{aligned} \boldsymbol{\mu}_k^{(j)} &= \sum_{i=1}^{N} w^{(j,i)} \, F_{k-1}^k(\boldsymbol{\xi}_{k-1}^{(j,i)}) \\ \boldsymbol{\Sigma}_{X_k^-}^{(j)} &= \sum_{i=1}^{N} w^{(j,i)} \left(F_{k-1}^k(\boldsymbol{\xi}_{k-1}^{(j,i)}) - \boldsymbol{\mu}_k^{(j)}\right) \cdot \\ &\qquad \left(F_{k-1}^k(\boldsymbol{\xi}_{k-1}^{(j,i)}) - \boldsymbol{\mu}_k^{(j)}\right)^T \,, \end{aligned} \quad (27)$$

where $\boldsymbol{\xi}_k^{(j,i)} = [\mathbf{x}_k^{(j,i)}, \mathbf{u}_k^{(j,i)}]^T$ are the roots of the multivariate Hermite polynomial and $w^{(j,i)}$ the corresponding quadrature weights for the j-th belief component [2].

2.3.3 Lower and Upper Expectations

In NA often the interest is to compute the expectation of a quantity ϕ connected to the uncertain state $\mathbb{E}_p[\phi(\mathbf{X}_k)]$. When the state distribution is epistemic, the value of such expectation depends on the epistemic parameter as well

$$\mathbb{E}_{p_{\lambda_k}}[\phi(\mathbf{X}_k)] = \int \phi(\mathbf{x}_k) p(\mathbf{x}_k|\mathbf{y}_{1:k}; \boldsymbol{\lambda}_k) d\mathbf{x}_k \,. \quad (28)$$

Hence, we can compute tight bounds on such expectation such that

$$\mathbb{E}_{p_{\lambda_k}} \in \left[\underline{\mathbb{E}}_{p_{\lambda_k}}, \overline{\mathbb{E}}_{p_{\lambda_k}}\right] \quad (29)$$

where

$$\begin{aligned} \underline{\mathbb{E}}_{p_{\lambda_k}} &= \min_{\lambda_k} \mathbb{E}_{p_{\lambda_k}}[\phi(\mathbf{X}_k)] \\ \overline{\mathbb{E}}_{p_{\lambda_k}} &= \max_{\lambda_k} \mathbb{E}_{p_{\lambda_k}}[\phi(\mathbf{X}_k)] \,. \end{aligned} \quad (30)$$

By plugging the variational form (19) in the expectation definition, we obtain

$$\begin{aligned} \mathbb{E}_{p_{\lambda_k}}[\phi(\mathbf{X}_k)] &= \int \phi(\mathbf{x}_k) \sum_{j=1}^{M} \lambda_{x_k|y_{1:k}}^{(j)} q^{(j)}(\mathbf{x}_k) d\mathbf{x}_k \\ &= \sum_{j=1}^{M} \lambda_{x_k|y_{1:k}}^{(j)} \int \phi(\mathbf{x}_k) q^{(j)}(\mathbf{x}_k) d\mathbf{x}_k \\ &= \sum_{j=1}^{M} \lambda_{x_k|y_{1:k}}^{(j)} \mathbb{E}_{q^{(j)}}[\phi(\mathbf{X}_k)] \,. \end{aligned} \quad (31)$$

Therefore, once the kernels expectations $\mathbb{E}_{q^{(j)}}[\phi(\mathbf{X}_k)]$ are computed, e.g. using Gauss-Hermite quadrature rules, the lower bound can be easily computed as the solution of a linear programming problem

$$\begin{aligned} \underline{\mathbb{E}}_{p_{\lambda_k}} = \min_{\lambda_k} & \sum_{j=1}^{M} \lambda_{x_k|y_{1:k}}^{(j)} \mathbb{E}_{q^{(j)}}[\phi(\mathbf{X}_k)] \\ \text{s.t.} & \sum_{j=1}^{M} \lambda_{x_k|y_{1:k}}^{(j)} = 1 \,. \end{aligned} \quad (32)$$

The same holds for the upper bound where a maximisation is performed in place of a minimisation. Plenty of efficient numerical routines exist to solve linear programming problems, e.g. MATLAB's *linprog*. In addition, because the linear programming problem is a subclass of convex optimisation, the found optimum is also granted to be globally optimum. Therefore, the chosen variational parameterisation makes it extremely efficient and robust to compute tight lower and upper expectations.

3. Test Case

In this section, the developed epistemic filtering is applied to the NA of one leg of the Europa Clipper tour [12] to quantify the Probability of Impact (PoI) during a close encounter with Jupiter's moon Europa.

3.1 Problem Definition

The scenario studied is represented in Figure 3. The trajectory starts spans two successive flybys with an apocenter impulsive manoeuvre to target the second flyby (E18) identified by the black square. The spacecraft trajectory and its deviations are depicted with dotted black lines, Europa's orbit with a dotted blue line, the observations with a dashed yellow line and the $\Delta\mathbf{v}$ manoeuvre with a green arrow. Hence, the spacecraft trajectory starts from a close flyby and the initial uncertainty is propagated until the apocentre while performing OD. The OD campaign is carried out with an 8 hours ON 8 hours OFF schedule to faithfully model the part-time availability of the tracking stations availability. The PoI is then computed by propagating the uncertainty after the $\Delta\mathbf{v}$, and its associated execution errors, to the nominal flyby time without performing additional OD. The PoI is computed in such a way to ensure spacecraft safety and environmental protection to Europa even in the event of a communication loss after the main manoeuvre. Also, the delivered PoI after the apocentre manoeuvre is usually the more critical measure because: this $\Delta\mathbf{v}$ brings the spacecraft close to the moon; it introduces the largest execution errors; the state uncertainty can grow severely during the long propagation time.

The whole trajectory lasts for 14 days. The motion is described in a Europa-centred inertial reference frame, specifically the mean equinox and ecliptic of J2000 (ECLIPJ2000) [1]. The spacecraft dynamics is a high-fidelity full-ephemeris one including the gravitational fields of Jupiter (central and J_2), of its moons Europa (central and J_2), Io, Ganymede and Callisto, and of the Sun. The dynamics is numerically propagated with the library jTOP [3].

The goal is to quantify tight bounds on the PoI at flyby $[\underline{\text{PoI}}, \overline{\text{PoI}}]$. The PoI is computed as the probability of the spacecraft minimum distance from Europa, at flyby E18, to be smaller or equal to the radius of Europa R_{EUR} written as

$$\text{PoI}(\boldsymbol{\lambda}_{E18}) = \int \mathbb{1}(\phi_{r_{E18}}(\mathbf{x}_{E18}) \leq R_{EUR}) \cdot p(\mathbf{x}_{E18}; \boldsymbol{\lambda}_{E18})\, d\mathbf{x}_{E18}\ , \tag{33}$$

where $\phi_{r_{E18}}(\mathbf{x}_{E18})$ is the function mapping the Cartesian state to the pericenter distance of the hyperbolic trajectory with respect to Europa, and $\mathbb{1}(\cdot)$ is the indicator function.

3.2 Uncertainty Model

The initial distribution $p(\mathbf{x}_0; \boldsymbol{\lambda}_0)$ is written in the Gaussian mixture form as

$$p(\mathbf{x}_0; \boldsymbol{\lambda}_0) = \sum_{j=1}^{M} \lambda_0^{(j)} \mathcal{N}(\mathbf{x}_0; \boldsymbol{\mu}_0, \boldsymbol{\Sigma}_0^{(j)}) \tag{34}$$

with interval-valued weights

$$\lambda_0^{(j)} = [0, 1]\ \ \forall j = 1, \ldots, M\ . \tag{35}$$

The mean is the same for all the components and it is the nominal initial state. The covariances are defined as

$$\boldsymbol{\Sigma}_0^{(j)} = \text{blkdiag}\Big(\lambda_{0-1}^{(j)}\, \boldsymbol{\Sigma}_0(1{:}3, 1{:}3), \lambda_{0-2}^{(j)}\, \boldsymbol{\Sigma}_0(4{:}6, 4{:}6)\Big)$$

where $\lambda_{0-1}^{(j)}, \lambda_{0-2}^{(j)} \in [0.5, 2.0]$ are two multipliers scaling the reference covariance $\boldsymbol{\Sigma}_0$, $\boldsymbol{\Sigma}_0(1{:}3, 1{:}3)$ and $\boldsymbol{\Sigma}_0(4{:}6, 4{:}6)$ indicate respectively the position block and the velocity block and the operator blkdiag indicates a block-diagonal matrix. Being the multipliers defined within $[0.5, 2.0]$, they encompass kernels with covariance from half up to double the extent of the reference one. The reference covariance is defined from the one in Radial Transversal Normal (RTN) components

$$\boldsymbol{\Sigma}_{RTN} = \text{diag}\Big([3.7^2, 5.3^2, 9.3^2, 2.3e\text{-}3^2, 3.4e\text{-}3^2, 5.9e\text{-}3^2]\Big) \tag{36}$$

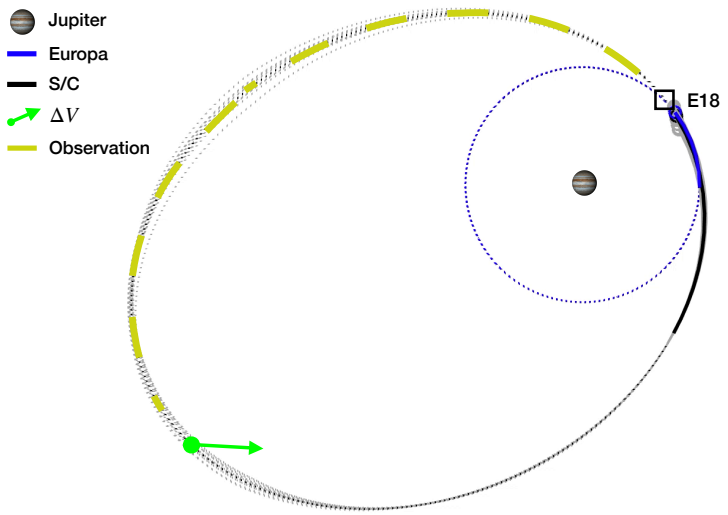

Fig. 3: Sketch of navigation analysis scenario for Europa Clipper leg.

where diag indicates a diagonal matrix and the unit of the first three elements is $[\mathrm{m}^2]$ while for the last three is $[\mathrm{m}^2/\mathrm{s}^2]$. Then, the reference covariance in inertial rectangular coordinates is computed as

$$\mathbf{\Sigma}_0 = \mathcal{J}_{RTN}^{Car}\mathbf{\Sigma}_{RTN}\mathcal{J}_{RTN}^{Car^T} \tag{37}$$

where $\mathcal{J}_{RTN}^{Car}$ is the Jacobian of the transformation from RTN to Cartesian coordinates.

The execution errors of the impulsive manoeuvre are modelled with Gates' model [5, 8], which decompose the additive error in magnitude (along the commanded $\Delta\mathbf{v}$ direction) and pointing components (perpendicular to the commanded $\Delta\mathbf{v}$ direction) as depicted in Figure 4. The parameters

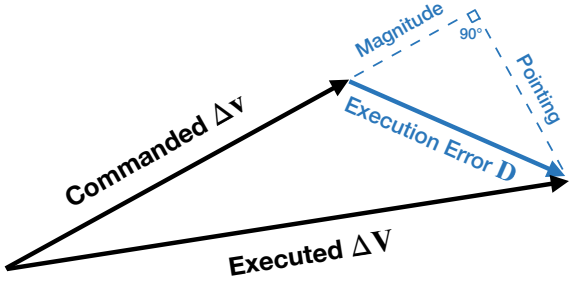

Fig. 4: Execution error by Gates' model.

of the Gates' model are reported in Table 1. This model has both fixed parameters, that is an error appears whenever a manoeuvre is performed, and proportional parameters, that is the error is larger for larger manoeuvres.

Table 1: Parameters Gates' model for execution errors.

Fixed Pointing σ_{pf}	3.33	[mm/s]
Proportional Pointing σ_{pp}	6.67	[mrad]
Fixed Magnitude σ_{mf}	4.67	[mm/s]
Proportional Magnitude σ_{mp}	0.33%	[-]

As for the OD, the tracking stations measure the spacecraft range and range-rate with respect to Earth [20]. The likelihood function is modelled as Gaussian mixture with epistemic coefficients as

$$p(\mathbf{y}_k|\mathbf{x}_k;\boldsymbol{\lambda}_y) = \sum_{j=1}^{M}\lambda_y^{(j)}\mathcal{N}(\mathbf{y}_k^{(j)};h(\mathbf{x}_k),\mathbf{\Sigma}_y) \tag{38}$$

where h is the range and range-rate observation model and the weights are interval-valued as

$$\lambda_y^{(j)} = [0,1] \;\; \forall j = 1,\ldots,M\,. \tag{39}$$

This time the covariance, quantifying the measurement accuracy, is fixed and set to

$$\mathbf{\Sigma}_y = \mathrm{diag}\Big([3.0^2, 0.1^2]\Big)\,, \tag{40}$$

where the unit of the range is $[\mathrm{m}^2]$ and for the range-rate is $[\mathrm{m}^2/\mathrm{s}^2]$. The exact value of the received measurement is unknown at the time of mission design, and therefore it is considered as an epistemic parameter $\mathbf{y}_k^{(j)}$.

The number of mixture components has been set to $M = 100$ for the initial distribution, the likelihood function and the variational distribution.

3.3 Navigation Analysis Results

The developed epistemic navigation analysis has been run on the described test case to robustly quantify the PoI range resulting from epistemic uncertainty. Figure 5 displays the resulting 3-σ uncertainty in B-plane coordinates at flyby E18. In detail, the several coloured ellipses result from different instances of the epistemic coefficients in the mixture representation. The equivalent Europa's surface is represented by the bold black line at $h = 0$ km, while the dashed grey ones represent Europa's subsurface for different depths. It can be seen that all the ellipses have a significant nonzero intersection with Europa's surface, but different instances of the epistemic parameters have a relevant influence on both the extension and the displacement of the uncertainty region.

The bounds on the PoI computed by Equation (32) using $\phi_{r_{E18}}$ are

$$\mathrm{PoI} \in [0.6, 6.5]\,\%\,. \tag{41}$$

The width of this interval indicate that epistemic uncertainty has a large effect on the value of the collision probability. In particular, epistemic uncertainty on the initial covariance and on the observation realisation has a large impact on the delivered uncertainty.

4. Conclusions

This paper presented novel developments in the field of navigation analysis under epistemic uncertainty as a fundamental step towards an integrated approach for trajectory design under generalised models of uncertainty. Specifically, the main contribution of this research is the introduction of a combination of variational inference and importance sampling to solve the Bayes' update step in the presence of epistemic priors and likelihoods.

The navigation analysis was framed as a sequential filtering problem dividing it into two fundamental steps: uncertainty propagation to map the state uncertainty distribution forward in time through the dynamical equations; orbit determination to update the state distribution incorporating the information coming from a received measurement. Then, methods for performing both these steps under epistemic mixture distributions were introduced and discussed. The OD step was solved by using the developed epistemic variational inference approach which requires the solution of several local optimisations to find the posterior distributions. The UP was realised by Gaussian Hermite quadrature rules sped up by sparse polynomial mappings to approximate the dynamical propagation.

Both the steps were solved maintaining the dynamical and observation nonlinearities and without enforcing restricting approximations or assumptions. Besides, such epistemic approach to navigation analysis allows one to include broader models of uncertainty and therefore to more faithfully characterise the uncertainty and information structure available during the different phases of mission design. Furthermore, the epistemic model removes the need for large Monte Carlo sampling over the initial dispersion, observation errors and model uncertainties. Another advantage of the developed approach is the formulation of lower and upper expectations as easy-to-solve linear programming problems.

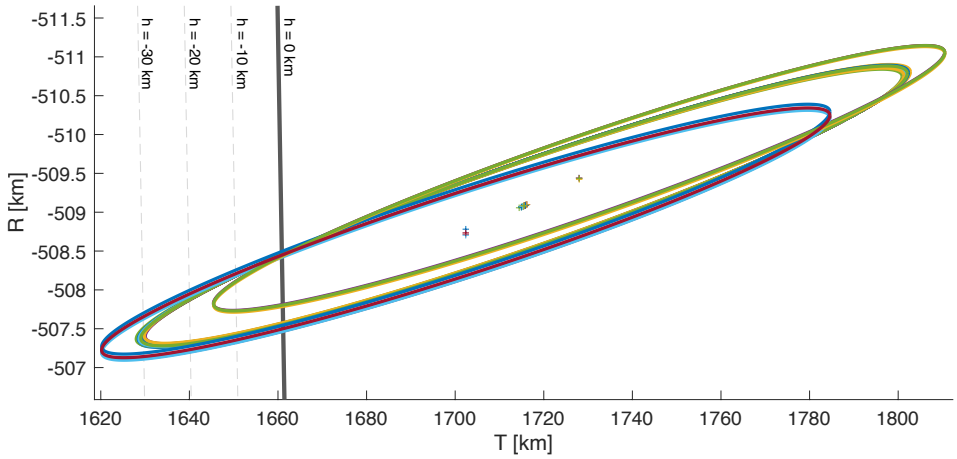

Fig. 5: Spacecraft 3-σ epistemic ellipses in B-plane coordinates.

The developed NA was finally applied to the robust quantification of collision probability bounds for Europa Clipper during one of its flybys with Jupiter's moon Europa. This test case encompassed epistemic uncertainty both on the initial dispersion and the observation likelihood, thus resulting in epistemic priors and posteriors along all the trajectory. OD arcs were performed before the main manoeuvre, which introduced executions errors as well, and then the PoI was quantified on the delivered uncertainty at the flyby. The range of PoI resulting from epistemic uncertainty was rather large, showing the importance of modelling and processing this systematic component as well in mission design. Indeed, in general, while the lower value $\underline{\text{PoI}}$ may be considered safe for some applications, the upper value $\overline{\text{PoI}}$ may not. A purely aleatoric approach, in which only precise distributions can be specified, would only be able to return a single value within the interval $[\underline{\text{PoI}}, \overline{\text{PoI}}]$, therefore providing only limited information to the mission designer.

As for the UP, future work will focus on an update routine for the mixture weights during propagation. In the OD step, future developments will revolve around the employment of different kernels which provide a more global coverage of the domain, such as Bernstein polynomials, as well as nonlinear epistemic parameters. A complexity analysis will then be performed to compare the numerical performance of this epistemic NA versus existing methods. Finally, future theoretical work will focus on the development of enhanced methods and proofs for constructing an epistemic posterior representation which conservatively approximates the infinite set of possible posteriors resulting from Bayes' inference.

Acknowledgements

This work was funded by the European Commission's H2020 programme, through the H2020-MSCA-ITN-2016 UTOPIAE Marie Curie Innovative Training Network, grant agreement no. 722734. The authors would like to thank Stefano Campagnola for his expert contribution in modelling the addressed application.

References

[1] Charles Acton, Nathaniel Bachman, Boris Semenov, and Edward Wright. A look towards the future in the handling of space science mission geometry. *Planetary and Space Science*, 150:9–12, 2018.

[2] J. Bäck, F. Nobile, L. Tamellini, and R. Tempone. Stochastic spectral Galerkin and collocation methods for PDEs with random coefficients: a numerical comparison. In J.S. Hesthaven and E.M. Ronquist, editors, *Spectral and High Order Methods for Partial Differential Equations*, volume 76 of *Lecture Notes in Computational Science and Engineering*, pages 43–62. Springer, 2011.

[3] S. Campagnola, N. Ozaki, Y. Sugimoto, C. H. Yam, H. Chen, Y. Kawabata, S. Ogura, B. Sarli, Y. Kawakatsu, R. Funase, and S. Nakasuka. Low-thrust trajectory design and operations of procyon, the first deep-space micro-spacecraft. In *24th International Symposium on Space Flight Dynamics*, Munich, Germany, 2015.

[4] Marilena Di Carlo, Massimiliano Vasile, Cristian Greco, and Richard Epenoy. Robust optimisation of low-thrust interplanetary transfers using evidence theory. In *29th AAS/AIAA Space Flight Mechanics Meeting*, pages 339–358, Ka'anapali, Hawaii, US, 2019. URL strathprints:67543.

[5] C. R. Gates. A simplified model of midcourse maneuver execution errors. Technical report, Jet Propulsion Laboratory, California Institute of Technology, 1963.

[6] Arthur Gelb. *Applied optimal estimation*. MIT press, 1974. Chap. 7.

[7] David K. Geller. Linear covariance techniques for orbital rendezvous analysis and autonomous onboard mission planning. *Journal of Guidance, Control, and Dynamics*, 29(6):1404–1414, 2006.

[8] Troy D Goodson. Execution-error modeling and analysis of the grail spacecraft pair. In *23rd AAS/AIAA Spaceflight Mechanics Meeting, Kauai, Hawaii*, 2013.

[9] Cristian Greco, Stefano Campagnola, and Massimiliano L Vasile. Robust space trajectory design using belief stochastic optimal control. In *AIAA Scitech 2020 Forum*, page 1471, 2020.

[10] Cristian Greco, Marilena Di Carlo, Massimiliano Vasile, and Richard Epenoy. Direct multiple shooting transcription with polynomial algebra for optimal control problems under uncertainty. *Acta Astronautica*, 170:224–234, 2020.

[11] E. D. Gustafson. *Stochastic Optimal Control of Spacecraft*. PhD thesis, The University of Michigan, 2010.

[12] Try Lam, Brent Buffington, and Stefano Campagnola. A robust mission tour for NASA's planned europa clipper mission. In *2018 Space Flight Mechanics Meeting*, page 0202, 2018.

[13] Sumita Nandi, Julie Kangas, Powtawche N. Valerino, Brent Buffington, Rodica Ionasescu, and Dylan Boone. Initial navigation analysis for the europa multiple flyby mission concept. In *26th AAS/AIAA Space Flight Mechanics Meeting*, 2016.

[14] J. T. Olympio. Designing robust low-thrust interplanetary trajectories subject to one temporary engine failure. In *20th AAS/AIAA Space Flight Meeting*, San Diego, CA, US, 2010.

[15] J. T. Olympio and C. H. Yam. Deterministic method for space trajectory design with mission margin constraints. In *61st International Astronautical Congress*, Prague, Czech Republic, 2010.

[16] N. Ozaki, S. Campagnola, R. Funase, and C. H. Yam. Stochastic differential dynamic programming with unscented transform for low-thrust trajectory design. *Journal of*

Guidance, Control, and Dynamics, 41:377–387, 2018.

[17] A. Richards and J. How. Robust stable model predictive control with constraint tightening. In *American Control Conference 2006 IEEE*, pages 6 pp.–, 2006.

[18] S. Sarkka. *Bayesian Filtering and Smoothing*. Cambridge University Press, New York, 1st edition, 2013.

[19] Nathan B. Stastny and David K. Geller. Autonomous optical navigation at jupiter: A linear covariance analysis. *Journal of Spacecraft and Rockets*, 45(2):290–298, 2008.

[20] Byron Tapley, Bob Schutz, and George H Born. *Statistical orbit determination*. Elsevier, 2004.

[21] Powtawche N. Valerino, Brent Buffington, Kevin Criddle, Yungsun Hahn, Rodica Ionasescu, Julie A. Kangas, Tomas Martin-Mur, Ralph B. Roncoli, and Jon A. Sims. Preliminary maneuver analysis for the europa clipper multiple-flyby mission. In *AIAA/AAS Astrodynamics Specialist Conference*, 2014.

[22] M. Vasile. Robustness optimisation of aerocapture trajectory design using a hybrid co-evolutionary approach. In *18th International Symposium on Space Flight Dynamics*, pages 1–6, Munich, Germany, 2004.

[23] F. Zuiani, M. Vasile, and A. Gibbings. Evidence-based robust design of deflection actions for near earth objects. *Celestial Mechanics and Dynamical Astronomy*, 114:107–136, 2012.